Supporting Information

Tang et al. 10.1073/pnas.1103015108

SI Materials and Methods

CatchER Biosensor Family Design Strategy. Based on key determinants for fine-tuning Ca^{2+} binding affinity and Ca^{2+}-induced conformational changes and the established chromophore properties of FPs, we hypothesized that Ca^{2+} sensors with a fast fluorescence response could be better designed by coupling Ca^{2+} binding sites directly to the chromophore rather than relying on stretched protein-protein interaction to modulate chromophore conformation. Our computationally assisted design is based on the following criteria and considerations. First, it requires four or five oxygen ligand atoms from protein residues (typically carboxyl groups of D, E, N, and Q) situated in the spherical geometry characteristic of natural Ca^{2+} binding proteins (1–5). Second, appropriate choice of residue charge and type can be made to fine-tune Ca^{2+} binding affinity and metal selectivity (6, 7). Third, diffusion-limited access of Ca^{2+} to the site requires good solvent accessibility (8). Fourth, propagating Ca^{2+}-induced local conformational and electrostatic changes to the chromophore can be achieved by properly locating the charged ligand residues with respect to the chromophore (9, 10). Fifth, these changes must occur rapidly, more quickly than the rate of conversion from a neutral to anionic state ascribed to these chromophores (11, 12). Sixth, the created binding site must not interfere with the chromophore's synthesis and formation. The EGFP variant with the M153T/V163A mutation (cycle 2) was chosen as the scaffold protein because of its high fluorescence intensity, folding efficiency, and thermostability (13).

Plasmid construction, protein expression, and purification. Bacterial expression plasmids for EGFP variants D8 to D12 were constructed by site-directed mutagenesis on cycle 2 EGFP (F64L/S65T/M153T/T163A) inserted in the pET28a vector (EMD Biosciences) between the BamHI and EcoRI restriction enzyme cleavage sites. The DNA sequence of the designed EGFP variants between these two restriction sites was cleaved and inserted into pcDNA3.1+ vector (Invitrogen). The calreticulin ER targeting sequence MLLSVPLLLGLLGLAAAD and ER retention sequence KDEL were added to the N and C termini, respectively, to construct the mammalian cell expression plasmids. EGFP variants were bacterially expressed in *Escherichia coli* BL21(DE3) following reported methods (11, 14).

Characterization of the optical properties of purified EGFP variants. The absorption spectra of EGFP variants were measured with a Shimadzu UV-1601 spectrophotometer. The protein concentration was determined at an absorption maximum of 280 nm with the coefficient 21,890 $cm^{-1}{\cdot}M^{-1}$ (11), and fluorescence spectra were determined (Photon Technology International, Inc.).

Cell culture and DNA transfection. C2C12 myoblasts were cultured in DMEM containing 4.5 g/L glucose (high glucose) with 2 mM L-glutamine plus 1.5 g/L sodium bicarbonate. CatchER plasmid DNA was transfected into these myoblasts by incubating the mixture of DNA and Lipofectamine 2000 at a ratio of 1:2 in Opti-MEM (Invitrogen) solution at 37 °C for 4 h. The transfection complex was replaced with fresh DMEM. Transfected cells were incubated at 30 °C and imaged after 48 or 72 h. A similar protocol was applied to HeLa, HEK-293, and BHK-21 cells.

Real-time fluorescence imaging. Real-time cell imaging was conducted on an inverted fluorescence microscope (DMI6000 B; Leica) with a cooled EM-CCD camera (C9100; Hamamatsu). The single-wavelength sensor was excited at 488 nm by a Xenon lamp (Polychrome V system; TILL PHOTONICS), with an HQ480/20× excitation filter, a 515DCXR dichromatic mirror, and a D535/25 emission filter (Chroma Technology Corporation). Fura-2 was excited alternatively at 340 nm with a D340xv2 excitation filter and at 380 nm with a D380xv2 filter, a 400DCLP dichromatic mirror, and a D510/80 emission filter. A perfusion system was used for drug application and solution exchange. Cells were imaged at 70% confluence. Intact cell imaging was conducted in Ringer buffer (121 mM NaCl, 2.4 mM K_2HPO_4, 0.4 mM KH_2PO_4, 1 mM Mg^{2+}, 10 mM Hepes) with or without 1.8 mM $CaCl_2$. Cells were permeabilized with 25 μM digitonin for 3–5 min and imaged in intracellular buffer (125 mM KCl, 25 mM NaCl, 10 mM Hepes, 0.5 mM Na_2ATP, 0.2 mM $MgCl_2$, 200 μM $CaCl_2$, 500 μM EGTA). The final amount of free [Ca^{2+}] was 100 nM (pH 7.25).

In situ measurement of CatchER's Ca^{2+} dissociation constant. CatchER's Ca^{2+} K_d was measured in BHK and C2C12 cells. ER Ca^{2+} in BHK cells was depleted by applying 100 μM histamine and 5 μM thapsigargin in Ringer 0 Ca^{2+} buffer. Cells were permeabilized in 100 μM digitonin in intracellular-like solution containing 140 mM KCl, 10 mM NaCl, 1 mM $MgCl_2$, 20 mM Hepes (pH 7.25) (15). Calibration buffers were prepared by adding Ca^{2+} to the intracellular-like solution, reaching final concentrations of 0.05, 0.1, 0.5, 1, 5, and 10 mM, and 200 μM EGTA buffer. Fluorescence at the lowest Ca^{2+} (F_{min}) and that at the highest Ca^{2+} (F_{max}) were determined in 200 μM EGTA and 10 mM Ca^{2+} with no Ca^{2+} ionophore, respectively.

Similar in situ K_d calibration was conducted in C2C12 myoblasts. ER Ca^{2+} of permeabilized cells was depleted in intracellular buffer containing 10 μM IP_3 and 2 μM thapsigargin. For calibration, 1, 3, 10, and 20 mM Ca^{2+} buffers were applied in the presence of 5 μM ionomycin. F_{min} and F_{max} were determined in 3 mM EGTA and 20 mM Ca^{2+}, respectively.

Fluorescence was normalized according to the equation:

$$f = \frac{F - F_{min}}{F_{max} - F_{min}}$$

and K_d was determined by the Hill equation:

$$f = \frac{[Ca^{2+}]^n}{K_d + [Ca^{2+}]^n}$$

K_d was 1.07 ± 0.26 mM (0.90 ± 0.19 Hill coefficient) in BHK-21 cells and 1.09 ± 0.20 mM (0.94 ± 0.17 Hill coefficient) in C2C12 cells.

Kinetic Analysis of Ca^{2+} Binding to CatchER by Stopped Flow. The fluorescence kinetics of bacterially expressed CatchER were investigated using an SF-61 stopped-flow spectrofluorometer (10-mm path length, 2.2-ms dead time at room temperature; Hi-Tech Scientific) at 22 °C. Fluorescence intensity changes were recorded with a 455-nm long-pass filter with excitation at 395 nm. Equal volumes of Ca^{2+}-free protein in 10 mM Tris-Cl (pH 7.4) and Ca^{2+} in the same buffer were mixed in the stopped-flow spectrofluorometer, yielding final concentrations of 10 μM CatchER and 50, 100, 200, 300, 500, and 1000 μM Ca^{2+}. The stopped-flow traces were fit to Eq. **S1**, which describes F, the fluorescence intensity, at any given time; F_{∞}, the fluorescence at infinite time; ΔF, the amplitude of the fluorescence change; k_{obs}, the observed rate constant; and t, the time.

$$F = F_{\infty} - \Delta F \exp(-k_{obs}{\cdot}t) \quad \textbf{[S1]}$$

$$F = F_{\infty} + \Delta F \exp(-k_{obs}{\cdot}t) \quad \textbf{[S2]}$$

$$k_{obs}\cdot\tau = \ln 2 \quad \textbf{[S3]}$$

Apparent pK_a determination by pH profile. The apparent pK_a of Ca^{2+}-free or Ca^{2+}-loaded CatchER was determined with bacterially expressed protein by fitting the fluorescence intensity change at 510 nm (λex = 488/395 nm). Protein (5 μM) was dissolved in different buffers, with pH ranging from 4.5 to 9.5 in the presence of either 10 μM EGTA (apo) or 4 mM Ca^{2+} (holo), and the actual pH was determined after measuring fluorescence. The proposed interaction scheme is

$$\mathbf{HP^+ \leftrightharpoons H^+ + P}$$

$$pH = pKa + \log\frac{[P]}{[HP^+]} \quad \textbf{[S4]}$$

$$f = \frac{F - F_{\min}}{F_{\max} - F_{\min}} \quad \textbf{[S5]}$$

$$F_{\min} = [P]_T c_1 \quad \textbf{[S6]}$$

$$F_{\max} = [P]_T c_2 \quad \textbf{[S7]}$$

$$F = ([P]_T - [P])c_1 + [P]c_2 \quad \textbf{[S8]}$$

$$f = \frac{[P]_T c_1 - [P]c_1 + [P]c_2 - [P]_T c_1}{[P]_T c_2 - [P]_T c_1} = \frac{[P]}{[P]_T} \quad \textbf{[S9]}$$

$$\frac{[P]}{[HP^+]} = \frac{1}{1/f - 1} \quad \textbf{[S10]}$$

$$f = \frac{1}{1 + \exp\left(\frac{pKa - pH}{c}\right)} \quad \textbf{[S11]}$$

H^+ is the proton; P is the CatchER protein; f is the normalized ΔF change; $[P]_T$ is the total protein concentration; c_1 or c_2 is the extinction coefficient of HP^+ or P fluorescence, respectively; F is the real-time fluorescence (fluorescence intensity); $F_{\min}$ is the fluorescence at the lowest pH; $F_{\max}$ is the fluorescence at the highest pH; and c is a constant for adjustment. The value theoretically equals log e. The apparent pK_a, fitted by a single exponential (Eq. **S11**), was 7.59 ± 0.03 and 6.91 ± 0.03 for apo and holo forms excited at 488 nm and 7.14 ± 0.02 and 6.95 ± 0.06 for apo and holo forms excited at 395 nm, respectively.

CatchER/Ca^{2+} stoichiometry studied by the Job Plot. The stoichiometry of the CatchER and Ca^{2+} interaction was determined at the maximal relative amount of Ca^{2+}-bound CatchER in the Job Plot (16). Ca^{2+}-free and -bound [CatchER] were converted to fluorescence intensity following the equation: $F = S_f\cdot C_f + S_b\cdot C_b$, where F is the apparent fluorescence intensity; S_f and S_b are the coefficients of Ca^{2+}-free and -bound CatchER, respectively; and C_f and C_b are the concentrations of Ca^{2+}-free and -bound CatchER, respectively. The relative amount of Ca^{2+}-bound CatchER ($C_b\cdot V$, $V = 1$) was calculated using Eq. **S12**. Fluorescence emission (λex = 488/395 nm) and absorbance spectra were recorded with [CatchER]: 28.7, 23.3, 19.4, 15.1, and 11.6 μM in response to [Ca^{2+}]: 11.3, 16.7, 20.6, 24.9, and 28.4 μM, respectively.

$$\frac{F_{Ca^{2+}-bound}}{F_{Ca^{2+}-free}} = \frac{S_f\cdot C_f + S_b\cdot C_b}{S_f\cdot C_T} = \frac{S_f(C_T - C_b) + S_b\cdot C_b}{S_f\cdot C_T} = 1 + \frac{C_b\cdot(S_b - S_f)}{S_f\cdot C_T} \quad \textbf{[S12]}$$

$$a = \frac{S_b - S_f}{S_f} \quad \textbf{[S13]}$$

$$\frac{C_b}{C_T}\cdot a = \frac{F_{Ca^{2+}-bound}}{F_{Ca^{2+}-free}} - 1 \quad \textbf{[S14]}$$

$$C_b\cdot V = \left(\frac{F_{Ca^{2+}-bound}}{F_{Ca^{2+}-free}} - 1\right)\cdot\frac{C_T}{a} \quad \textbf{[S15]}$$

NMR spectroscopy. All NMR experiments were performed at 37 °C using a Varian 800- or 600-MHz spectrometer. Typically, NMR samples contained 0.3 mM ^{15}N- or ^{13}C, ^{15}N-labeled protein in 10 mM Tris, 10 mM KCl, 10% (vol/vol) D_2O (pH 7.4). Data were processed using NMRpipe (17) and analyzed with the program Sparky (T. D. Goddard and D. G. Kneller, University of California, San Francisco). For backbone assignment of ^1H, ^{13}C, and ^{15}N resonances, an experiment correlating the amide ^1H and ^{15}N chemical shifts with the intraresidue $^{13}C\alpha$ (HNCA) was collected on a Varian Inova 800-MHz spectrometer, and an experiment correlating $^{13}C\beta$ and $^{13}C\alpha$ resonances of a residue with the ^{15}N and ^1H resonances of the following residue [CBCA(CO)NH] was collected on a Varian Inova 600-MHz spectrometer, both equipped with a cryogenic probe. For Ca^{2+} titration, {^1H, ^{15}N} HSQC spectra were collected and chemical shift perturbations were calculated using the equation $\Delta\delta_{av} = \{0.5[\Delta\delta(^1H^N)^2 + (0.2\ \Delta\delta(^{15}N))^2]\}^{1/2}$, where $\Delta\delta$ is the change in chemical shift between the apo and Ca^{2+}-loaded forms. Rotational correlation time (τ_c) was measured using a shared, constant-time, cross-correlated relaxation pulse sequence developed by the Prestegard laboratory (18). In this measurement, a series of highly sensitive HSQC spectra were collected at relaxational acquisition times from 0 to ~100 ms. Residue-specific τ_c values were then extracted from the exponential decay rates (19). T_1 and T_2 were collected on a Varian Inova 600-MHz spectrometer. Integrations of peak collected at 0, 30, 60, 100, 240, 480, 720, 1,000, and 1,500 ms (T_1) and 10, 30, 50, 70, 90, 110, 130, and 150 ms (T_2) were fitted with $I = I_0 exp(-t/T_{1/2})$, where I_0 is the intensity at zero decay and t is the relaxation decay. The τ_c values were calculated based on the following equations:

$$\tau_c = (2\omega_N)^{-1}\cdot\sqrt{(6T_1/T_2 - 7)} \quad \textbf{[S16]}$$

$$\omega_N = 2\pi\cdot f_N \quad \textbf{[S17]}$$

Adult mouse myofiber electrophysiological and optical recordings. Single skeletal muscle fibers from the flexor digitorum brevis (FDB) were obtained from Freund Virus B (FVB) mice raised in the Animal Research Program of Wake Forest University School of Medicine (WFUSM) at 3–5 mo (young) or 22–25 mo (old). They were killed by cervical dislocation. Animal handling followed a protocol approved by the WFUSM Animal Care and Use Committee.

The pcDNA3.1 plasmid carrying CatchER was electroporated in vivo into the FDB muscle. FDB fibers were enzymatically dissociated 3 to 4 wk after muscle electroporation, as described elsewhere (20). Solutions used for whole-cell patch-clamp and field stimulation recordings are described elsewhere (21, 22). High EGTA (20 mM) was used in the pipette solution to reproduce experimental conditions in a series of studies on FDB muscle fibers in which SR Ca^{2+} release was recorded in the cytosol (21). For field stimulation recordings, FDB fibers were

loaded with 250 μM EGTA. These procedures prevent Rhod-2 saturation without modifying SR Ca^{2+} kinetics release (data not shown). Fluorescence signals were recorded using a Radiance 2100 (Bio-Rad, Zeiss) confocal system in the line-scan mode and converted to intensity profiles using ImageJ software (National Institutes of Health).

CatchER calibration in FDB fibers. CatchER fluorescence was transformed into Ca^{2+} concentration according to the equation $[Ca^{2+}]_i = K_d(F - F_{min})/(F_{max} - F)$ (23). The K_d value was calculated in enzymatically dissociated FDB fibers, as reported (25), with some modifications. Fibers from young and old mice expressing CatchER were exposed to 0.01% saponin for ~2 min in a solution containing 90 mM K-glutamate, 1.02 mM $MgCl_2$, 5 mM NaCl, 10 mM Hepes, 1 mM 1,2-bis(*o*-aminophenoxy)ethane-n,n,n′,n′-tetraacetic acid (BAPTA), 0.323 mM $CaCl_2$, 0.025 *N*-benzyl-p-toluene sulphonamide (BTS), 2% (vol/vol) poly (*N*-vinyl-2-pyrrolidone) (PVP) (1 mM free Mg^{2+}, 0.0001 mM free Ca^{2+}) (pH 7.2), adjusted with KOH. The permeabilized myofiber was exposed to 10^{-6} M ionomycin diluted in the previous solution to equilibrate various free Ca^{2+} concentrations among the extracellular space, cytosol, and lumen of the SR. For all solutions, free $[Mg^{2+}]$ was set at 1 mM and free $[Ca^{2+}]$ was set at concentrations ranging from 10^{-7} to 10^{-1} M by buffering with BAPTA, as calculated by the Max-Chelator program. CatchER's F_{min} and F_{max} were measured in each fiber for which we reported the SR resting Ca^{2+} concentration. CatchER's K_d measured in FDB fibers from young and old mice was 1.66 ± 0.08 mM and 1.71 ± 0.12 mM, respectively. Fluorescence recorded after fiber exposure to 0.01% saponin in 100 nM Ca^{2+} solution (no ionomycin added), pCa ($-\log[Ca^{2+}]$) 7 plus ionomycin, or pCa 1 plus ionomycin was considered to calculate resting fluorescence (F_{rest}), F_{max}, and F_{min}, respectively. The F_{min} value was confirmed by adding 1 mM 4-CmC to fibers incubated in 100 nM Ca^{2+} plus ionomycin. The ratio between the fluorescence recorded in the presence of cresol and 100 nM Ca^{2+} plus ionomycin was 1.06 ± 0.01 (n = 5). Fibers were imaged in the x-y mode of the confocal microscope 1 min after solution exchange or until SR fluorescence reached a steady value.

1. Khan F, Stott K, Jackson S (2003) ^{1}H, ^{15}N and ^{13}C backbone assignment of the green fluorescent protein (GFP). *J Biomol NMR* 26:281–282.
2. Yang W, et al. (2003) Rational design of a calcium-binding protein. *J Am Chem Soc* 125:6165–6171.
3. Kirberger M, et al. (2008) Statistical analysis of structural characteristics of protein Ca^{2+}-binding sites. *J Biol Inorg Chem* 13:1169–1181.
4. Wang X, Kirberger M, Qiu F, Chen G, Yang JJ (2009) Towards predicting Ca^{2+}-binding sites with different coordination numbers in proteins with atomic resolution. *Proteins* 75:787–798.
5. Wang X, et al. (2010) Analysis and prediction of calcium-binding pockets from apo-protein structures exhibiting calcium-induced localized conformational changes. *Protein Sci* 19:1180–1190.
6. Jones LM, et al. (2008) Rational design of a novel calcium-binding site adjacent to the ligand-binding site on CD2 increases its CD48 affinity. *Protein Sci* 17:439–449.
7. Maniccia AW, Yang W, Li SY, Johnson JA, Yang JJ (2006) Using protein design to dissect the effect of charged residues on metal binding and protein stability. *Biochemistry* 45:5848–5856.
8. Barondeau DP, Kassmann CJ, Tainer JA, Getzoff ED (2002) Structural chemistry of a green fluorescent protein Zn biosensor. *J Am Chem Soc* 124:3522–3524.
9. Li S, et al. (2008) Rational design of a conformation-switchable Ca^{2+}- and Tb^{3+}-binding protein without the use of multiple coupled metal-binding sites. *FEBS J* 275:5048–5061.
10. Bizzarri AR, Cannistraro S (2007) Statistical analysis of intensity fluctuations in single molecule SERS spectra. *Phys Chem Chem Phys* 9:5315–5319.
11. Zou J, et al. (2007) Developing sensors for real-time measurement of high Ca^{2+} concentrations. *Biochemistry* 46:12275–12288.
12. Abbruzzetti S, et al. (2005) Kinetics of acid-induced spectral changes in the GFPmut2 chromophore. *J Am Chem Soc* 127:626–635.
13. Fukuda H, Arai M, Kuwajima K (2000) Folding of green fluorescent protein and the cycle3 mutant. *Biochemistry* 39:12025–12032.
14. Miyawaki A, et al. (1997) Fluorescent indicators for Ca^{2+} based on green fluorescent proteins and calmodulin. *Nature* 388:882–887.
15. Rudolf R, Magalhães PJ, Pozzan T (2006) Direct in vivo monitoring of sarcoplasmic reticulum Ca^{2+} and cytosolic cAMP dynamics in mouse skeletal muscle. *J Cell Biol* 173:187–193.
16. Huang CY (1982) Determination of binding stoichiometry by the continuous variation method: The Job plot. *Methods Enzymol* 87:509–525.
17. Delaglio F, et al. (1995) NMRPipe: A multidimensional spectral processing system based on UNIX pipes. *J Biomol NMR* 6:277–293.
18. Liu Y, Prestegard JH (2008) Direct measurement of dipole-dipole/CSA cross-correlated relaxation by a constant-time experiment. *J Magn Reson* 193:23–31.
19. Lee HW, et al. (2002) Isolated EF-loop III of calmodulin in a scaffold protein remains unpaired in solution using pulsed-field-gradient NMR spectroscopy. *Biochim Biophys Acta* 1598:80–87.
20. Wang Z-M, Messi ML, Renganathan M, Delbono O (1999) Insulin-like growth factor-1 enhances rat skeletal muscle L-type Ca^{2+} channel function by activating gene expression. *J Physiol* 516:331–341.
21. Jiménez-Moreno R, Wang ZM, Messi ML, Delbono O (2010) Sarcoplasmic reticulum Ca^{2+} depletion in adult skeletal muscle fibres measured with the biosensor D1ER. *Pflugers Arch* 459:725–735.
22. Payne AM, Jimenez-Moreno R, Wang ZM, Messi ML, Delbono O (2009) Role of Ca^{2+}, membrane excitability, and Ca^{2+} stores in failing muscle contraction with aging. *Exp Gerontol* 44:261–273.
23. Tsien RY, Pozzan T (1989) Measurement of cytosolic free Ca^{2+} with quin2. *Methods Enzymol* 172:230–262.
24. Bryant DT, Andrews P (1984) High-affinity binding of Ca^{2+} to bovine alpha-lactalbumin in the absence and presence of EGTA. *Biochem J* 220:617–620.
25. Ziman AP, Ward CW, Rodney GG, Lederer WJ, Bloch RJ (2010) Quantitative measurement of Ca^{2+} in the sarcoplasmic reticulum lumen of mammalian skeletal muscle. *Biophys J* 99:2705–2714.

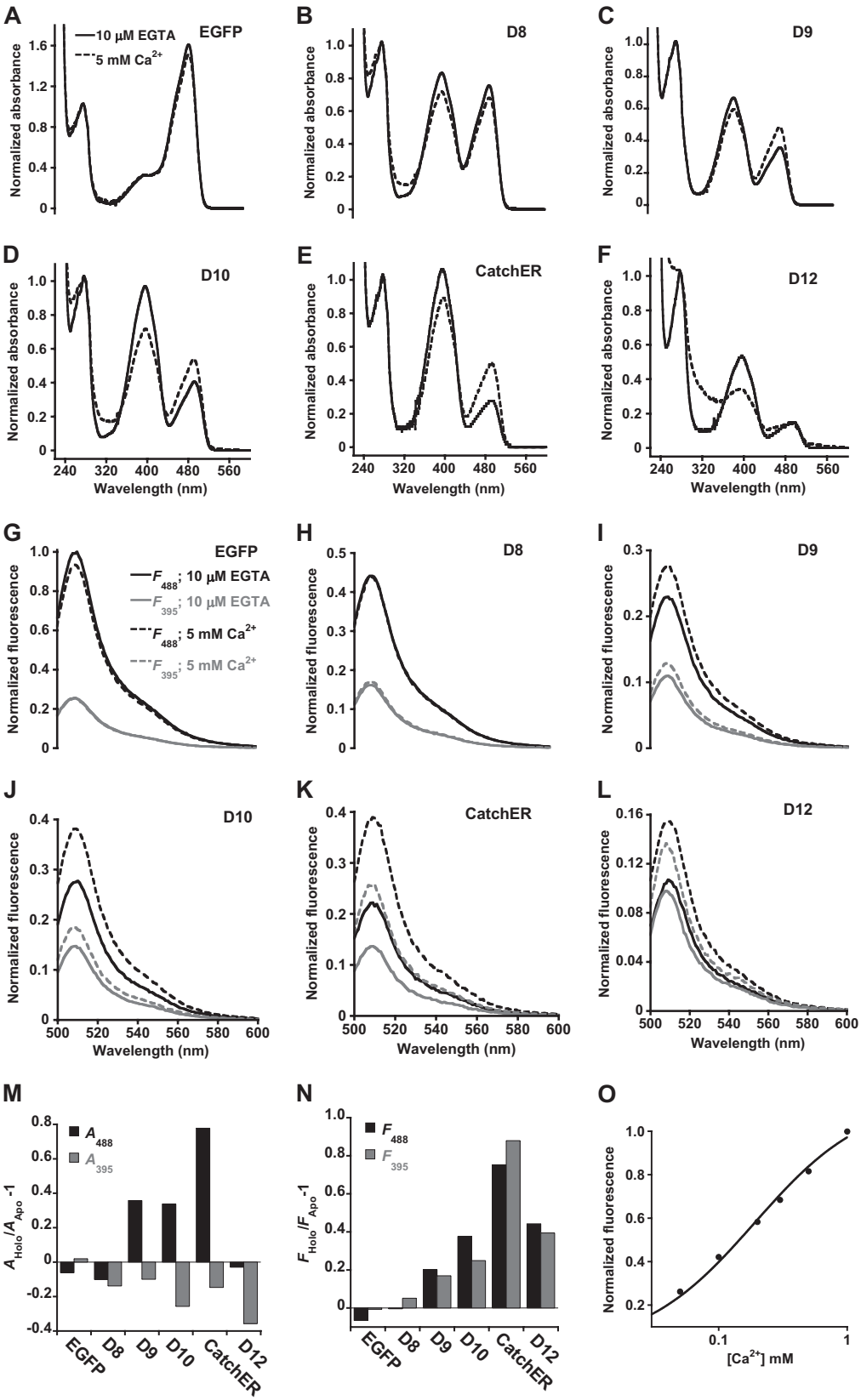

Fig. S1. Fluorescence and absorbance change of purified, bacterially expressed, designed EGFP-based sensors in response to Ca^{2+} detected by an UV or fluorescence spectrophotometer to demonstrate that the dynamic range of the sensors can be rationally tuned. (*A*) Overlaid absorbance spectra from 220 to 600 nm of EGFP measured by a UV spectrophotometer in the presence of 10 μM EGTA (solid line) or 5 mM Ca^{2+} (dashed line). (*B–F*) Absorbance spectra of designed EGFP-based sensors D8, D9, D10, CatchER, and D12 (schemes of design and names of these variants are shown in Fig. 1 *C–H*), respectively, measured in

Legend continued on following page

the same way as EGFP shown in *A*. The axis of absorption wavelength of EGFP, D8, and D9 in *A*–*C* is not shown but correlated to D10, CatchER, and D12, respectively, in *D*–*F*. The absorbance maximal at 488 nm increased and that at 395 nm decreased in D9, D10, and CatchER (*C*–*E*) in response to Ca^{2+}. (*G*) Overlaid fluorescence emission spectra from 500 to 600 nm of EGFP measured by a fluorometer in the presence of 10 μM EGTA (solid line) or 5 mM Ca^{2+} (dashed line) with the same sample corresponding to *A*. The two overlaid emission spectra (black) on the top were excited at 488 nm, and the two on the bottom were excited at 395 nm (gray). (*H*–*L*) Fluorescent emission spectra of designed EGFP-based sensors D8, D9, D10, CatchER, and D12, respectively, measured in the same way as EGFP in *G*. The axis of absorption wavelength of EGFP, D8, and D9 in *G*–*I* is not shown but correlated to D10, CatchER, and D12, respectively, in *J*–*L*. (*M*) Comparison of the amplitudes of absorbance change at 488 nm (black bar) and 395 nm (gray bar) of EGFP and designed variants in response to Ca^{2+} to original spectra in *A*–*F*. The amplitude change is in the term of ($A_{Holo}/A_{Apo}-1$) and A_{Holo} and A_{Apo} represent the absorbance intensity in the presence of 5 mM Ca^{2+} and 10 μM EGTA, respectively. The ratiometric absorbance change at 488 and 395 nm of D9, D10, and CatchER in response to Ca^{2+} is presented in the positive and negative values of the bars, respectively. (*N*) Comparison of the amplitudes of fluorescence emission change at 510 nm excited at 488 nm (black bar) and 395 nm (gray bar) of EGFP and designed variants in response to Ca^{2+} with the original spectra in *G*–*L*. The amplitude change is in the term of ($F_{Holo}/F_{Apo}-1$), and F_{Holo} and F_{Apo} represent the absorbance intensity in the presence of 5 mM Ca^{2+} and 10 μM EGTA, respectively. The nonratiometric fluorescence change at 510 nm excited at either 488 or 395 nm of D9, D10, CatchER, and D12 is presented in the positive values of the bars. Absorbance at 280 nm of all the variants was normalized to 1. (*O*) Final fluorescence intensity (F_∞) of the stopped-flow experiment (Fig. 2*D*) in the function of [Ca^{2+}] was fitted by a 1:1 binding mode with a calculated K_d of 0.19 mM.

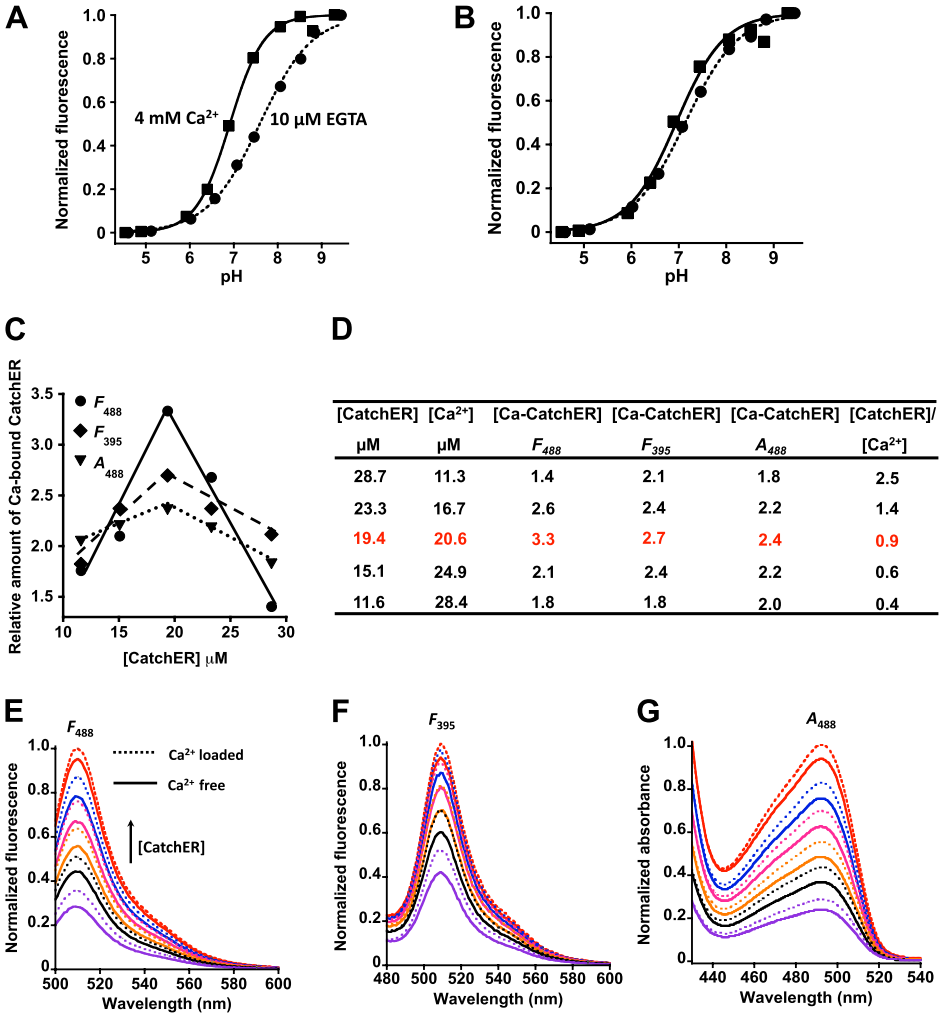

[CatchER] μM	[Ca^{2+}] μM	[Ca-CatchER] F_{488}	[Ca-CatchER] F_{395}	[Ca-CatchER] A_{488}	[CatchER]/[Ca^{2+}]
28.7	11.3	1.4	2.1	1.8	2.5
23.3	16.7	2.6	2.4	2.2	1.4
19.4	20.6	3.3	2.7	2.4	0.9
15.1	24.9	2.1	2.4	2.2	0.6
11.6	28.4	1.8	1.8	2.0	0.4

Fig. S2. pH stability of CatchER before and after binding Ca^{2+} is investigated by measuring the apparent pK_a values based on pH dependence of the fluorescence intensity, and the stoichiometric interaction between CatchER and Ca^{2+} is determined by Job's Plot. (*A*) Fluorescence emission intensities at 510 nm were recorded in the presence of 10 μM EGTA (●) or 4 mM Ca^{2+} (■) with excitation at 488 nm at corresponding pH values. The apparent pK_a is calculated with the fitting equations in *SI Materials and Methods* to be 7.59 ± 0.03 (EGTA) and 6.91 ± 0.03 (Ca^{2+}). (*B*) pH dependence of the fluorescence emission intensities at 510 nm excited at 395 nm were recorded and fitted with the same methods used in *A*. The apparent pK_as are 7.14 ± 0.02 (EGTA) and 6.95 ± 0.06 (Ca^{2+}). (*C*) Job's Plot of the relative amount of Ca^{2+}-bound CatchER as determined by fluorescence (F_{488}, F_{395}) and absorbance (A_{488}) as a function of [CatchER]. (*D*) Numerical results of the Job Plot in *C*. Fluorescent spectra with [CatchER] of 28.7, 23.3, 19.4, 15.1, and 11.6 μM (solid line) in response to [Ca^{2+}] = 11.3, 16.7, 20.6, 24.9, and 28.4 μM (dashed line), excited at 488 nm (*E*) or 395 nm (*F*). (*G*) Corresponding absorbance change in the absence (solid line) or presence (dashed line) of Ca^{2+}.

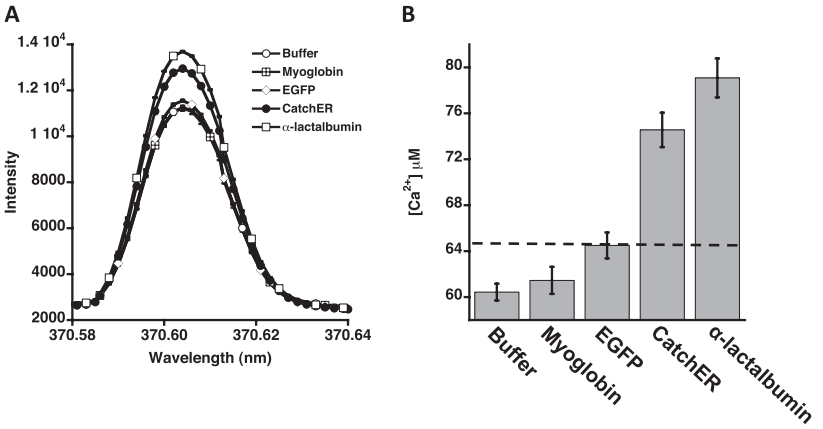

Fig. S3. Ca^{2+} binding CatchER investigated by equilibrium dialysis and an inductively coupled plasma optical emission spectrometer (ICP-OES). Dialysis tubes contained 6 mL of myoglobin (Sigma Chemical Co.) (non–Ca^{2+}-binding protein), EGFP (non–Ca^{2+}-binding protein), CatchER, and α-lactalbumin (Sigma Chemical Co.) [Ca^{2+}-binding protein with reported $K_d = 10^{-9}$ M (24)] at a concentration of 20 μM determined before dialysis, floating inside a beaker containing 1,800 mL of 10 mM Tris buffer with Ca^{2+} (pH 7.4). The ICP-OES provides a sensitive method of determining the total concentration of a particular metal in solution with high selectivity. (*A*) Representative spectra of the ICP-OES to determine the total Ca^{2+} concentration (both bound and unbound) outside the dialysis tube (buffer) and inside the dialysis tube with the samples of myoglobin, EGFP, CatchER, and α-lactalbumin, respectively, with maximal intensity at 370.602 nm. Each spectrum is the average of three time repeats with the error bars, and the amplitude of peak intensity of each sample represents the concentration of Ca^{2+}. (*B*) Comparison of Ca^{2+} concentration of each sample determined by the ICP-OES. The peak intensities recorded at 396.847, 373.690, 219.779, 370.602, 317.933, 643.907, and 220.861 nm were converted to Ca^{2+} concentration calibrated by the predetermined Ca^{2+} standard linear curve at each wavelength, respectively. The Ca^{2+} concentration of the buffer outside the dialysis tube was 60.4 ± 0.7 μM (unbound), and that inside the dialysis tube (both bound and unbound), containing myoglobin, EGFP, CatchER, and α-lactalbumin, was 61.5 ± 1.2, 64.5 ± 1.1, 74.6 ± 1.5, and 79.1 ± 1.7 μM (both bound and unbound), respectively.

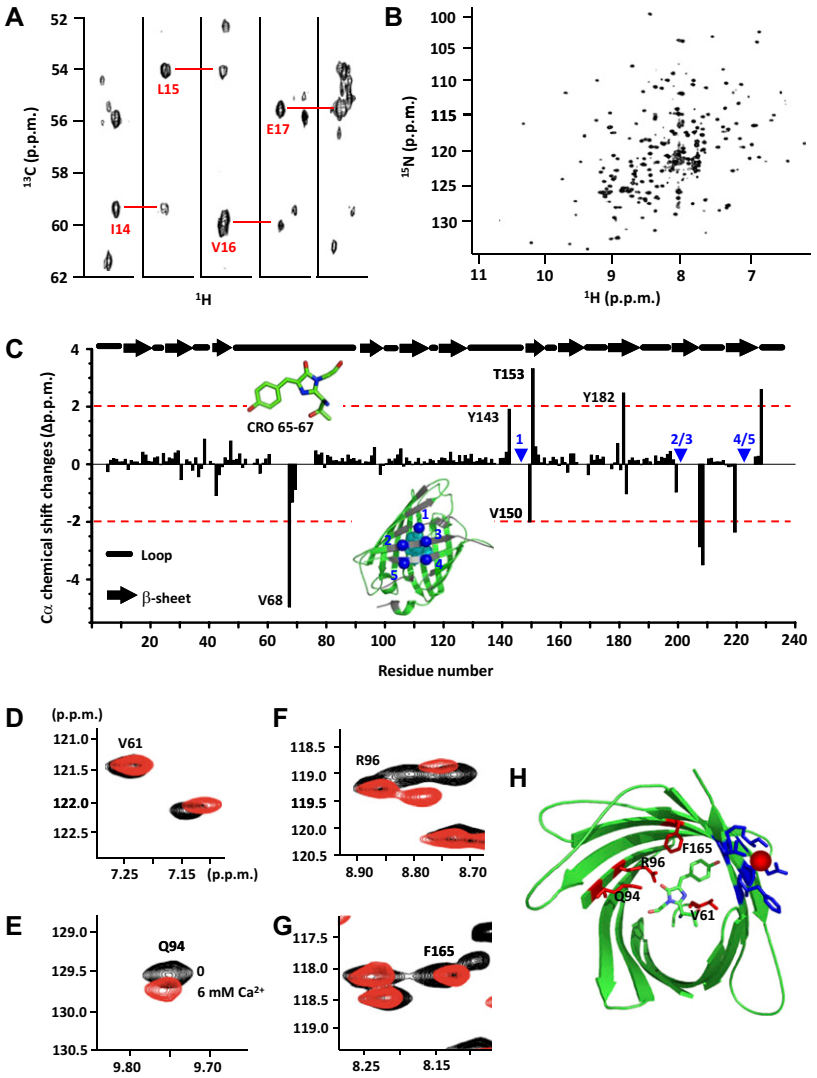

Fig. S4. CatchER NMR assignment and subtle Ca^{2+} influence on the residues interacting with the chromophore on the opposite side of the designed Ca^{2+} binding site. (*A*) Selected CatchER 3D HNCA spectra from I14 to E17, with sequential and intraresidual Cα-Cα connections indicated by red lines. (*B*) CatchER 2D {^{1}H-^{15}N} HSQC spectrum. (*C*) Difference in Cα chemical shift between published data (1) and our data. Most labeled residues exhibiting more than a 1.5-ppm chemical shift difference were sequentially close to the chromophore or the designed Ca^{2+} binding site (blue). The numbers 1–5 represent E147, D202, E204, E223, and E225, respectively. Unassigned CatchER residues are gray in the structure. All the data were recorded at 37 °C using an 800-MHz NMR spectrometer with a cryogenic probe and a 300-mM ^{13}C-^{15}N double-labeled sample in 10 mM Tris (pH 7.4). (*D*–*G*) CatchER 2D {^{1}H-^{15}N} HSQC spectrum recorded at 0 mM Ca^{2+} (black) and 6 mM Ca^{2+} (red). A subtle chemical shift change was observed for Q94 at 6 mM Ca^{2+}, but no change was observed for R96, F165, or V61. (*H*) Side chains of R96, Q94, F165, and V61 (red) protruded toward the chromophore (green sticks) on the opposite side of the designed Ca^{2+} binding site (blue). All data were recorded at 37 °C using a 600-MHz NMR spectrometer with a 300-μM ^{15}N-labeled sample in 10 mM Tris and 10 mM KCl (pH 7.4).

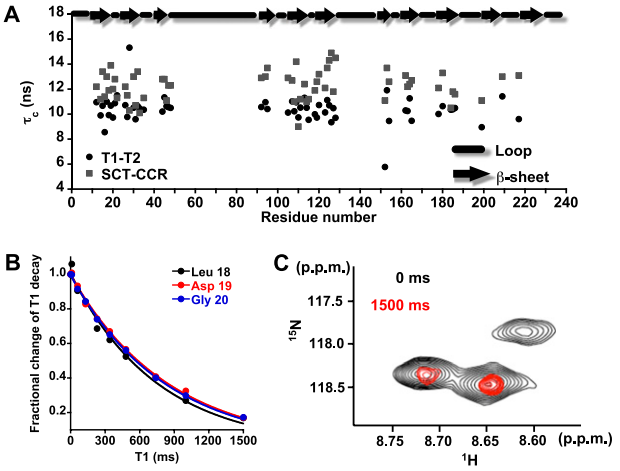

Fig. S5. Monomerization of CatchER is supported by the measured rotational correlation time, τ_C, with high-field NMR spectroscopy. (*A*) τ_C directly determined by the shared, constant-time, cross-correlated relaxation (SCT-CCR) experiment performed on an 800-MHz NMR spectrometer (gray squares) or calculated using Eqs. **S16** and **S17** with relaxation times T_1 and T_2 determined on a 600-MHz NMR spectrometer (●) (*SI Materials and Methods*). The secondary structures of corresponding residues are marked above. (*B*) Representative fitting of peak integrations collected at 0-, 30-, 60-, 100-, 240-, 480-, 720-, 1,000-, and 1,500-ms T_1 delays. (*C*) Overlay of T_1 delay spectra from selected region: 0 ms (black), 1,500 ms (red).

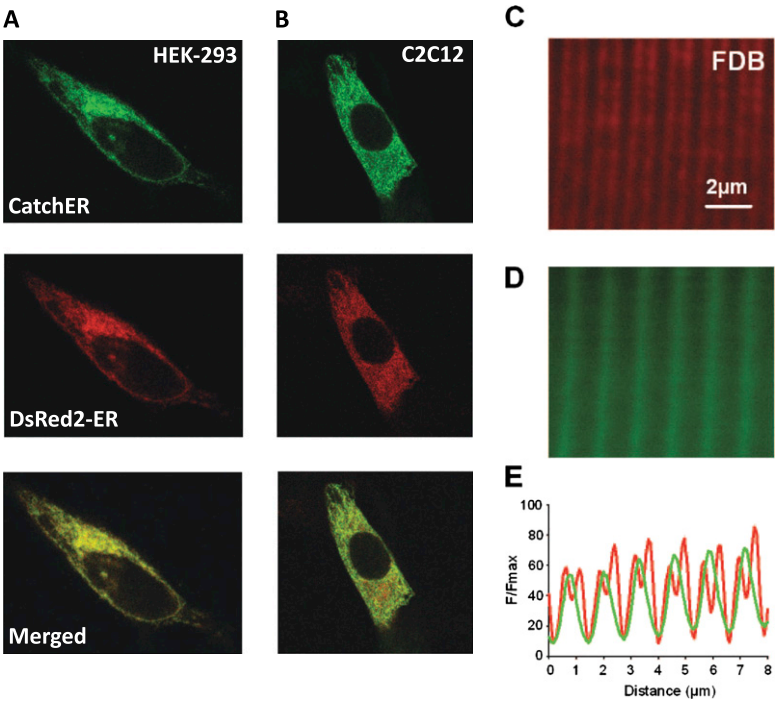

Fig. S6. Localization of CatchER expressed in the ER of HEK-293 and C2C12 cells and the SR of FDB fibers. Colocalization of CatchER and DsRed2-ER (BD Biosciences, Clontech) in HEK-293 (*A*) and C2C12 (*B*) cells. CatchER (green) and DsRed2-ER (red) were transiently cotransfected and expressed in two cell lines for confocal microscopy imaging. The overlay imaging shows the colocalization of CatchER corresponding to ER-tracker DsRed2-ER. Fiber expressing CatchER stained with di-8-ANEPPS [one of the ANEP (AminoNaphthyEthenylPyridinium) class of membrane potential dyes] and imaged with a confocal microscope (*C*) shows a striation pattern corresponding to the t-tubule. (*D*) CatchER fluorescence. (*E*) Normalized fluorescence intensity profiles for CatchER and di-8-ANEPPS measured in the area shown in *D*.

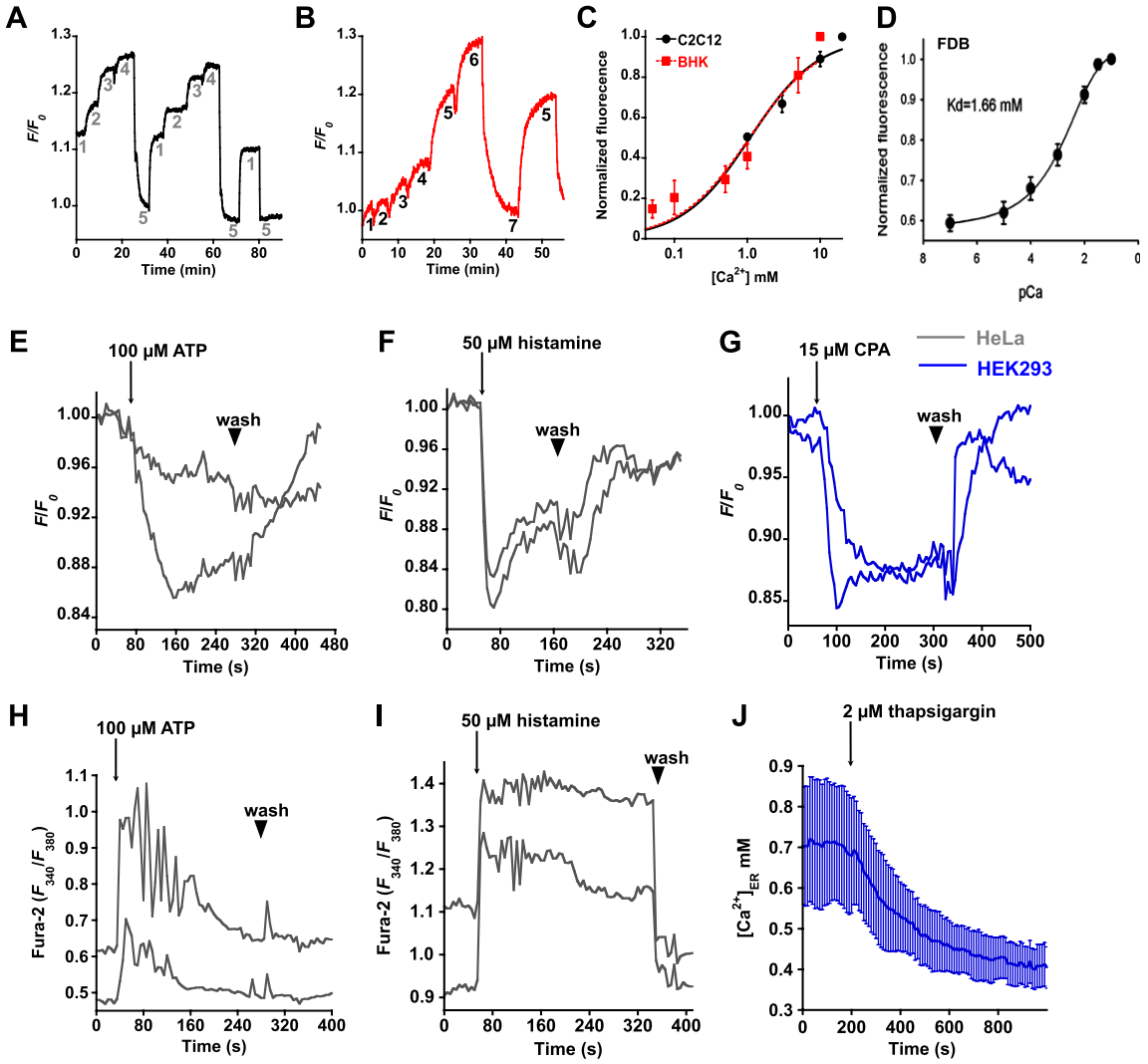

Fig. S7. In situ determination of K_d and ER Ca^{2+} dynamics of HeLa and HEK-293 cells. (*A*) In situ determination of K_d in ER of C2C12 myoblast cells. The numbers 1–5 correspond to 1, 3, 10, and 20 mM Ca^{2+} and 3 mM EGTA, respectively. (*B*) K_d determination in BHK-21 cells. The numbers 1–7 represent 0.05, 0.1, 0.5, 1, 5, and 10 mM Ca^{2+} and 200 μM EGTA, respectively. CatchER fluorescent signals of transfected permeabilized cells after equilibration with various extracellular Ca^{2+} concentrations excited at 488 nm are shown. (*C*) K_d calculation with a 1:1 binding mode. (*D*) Calibration of CatchER's K_d in FDB fibers. CatchER's fluorescence recorded in FDB fibers from young mice was normalized and plotted as a function of a wide range of pCa values (*SI Materials and Methods*). Experimental points were fitted to a Hill equation, and the K_d value was calculated. Representative ER Ca^{2+} signaling was detected by CatchER in HeLa cells triggered by ATP (*E*) and histamine (*F*), and corresponding cytosolic Ca^{2+} signaling was measured with Fura-2 in separated cells (*H* and *I*) using the same protocol. (*G*) Reversible Ca^{2+} release triggered by 15 μM cyclopiazonic acid (CPA) in HEK-293 cells. (*J*) Quantification of irreversible ER Ca^{2+} release in HEK-293 cells induced by 2 μM thapsigargin in the presence of 1 mM extracellular Ca^{2+}. F_{min} and F_{max} were determined by adding 5 mM EGTA and 50 mM Ca^{2+}, respectively, to the intact cells in the presence of 5 μM ionomycin (n = 6).

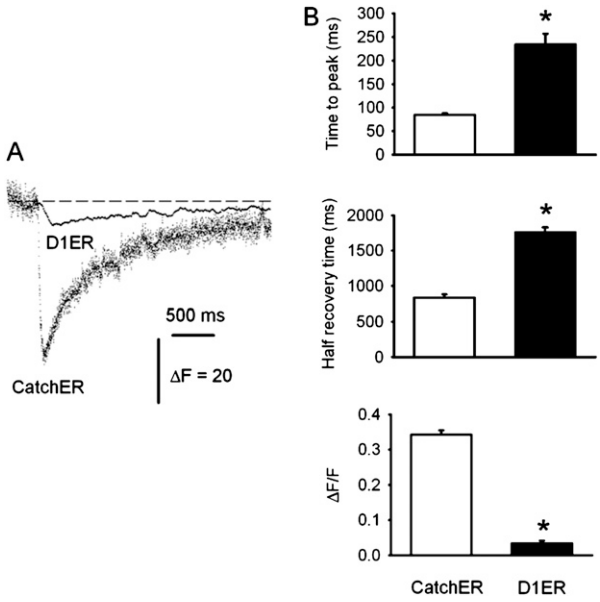

Fig. S8. CatchER and D1ER Ca^{2+} release and uptake kinetics in response to muscle fiber depolarization. (*A*) SR Ca^{2+} transients were recorded in FDB fibers expressing either CatchER or D1ER elicited by 100-ms command pulses to 20 mV under whole-cell patch-clamp. CatchER's and D1ER citrine's fluorescence is illustrated to compare their amplitude and kinetics. D1ER citrine emission (535 nm) was chosen over the cyan fluorescence protein (485 nm) because of its larger amplitude. The D1ER excitation wavelength was set at 436 nm. D1ER's and CatchER's fluorescence was recorded using a spectrofluorometer and confocal microscope in the line-scan mode (see above), respectively. The dashed line indicates the baseline. (*B*) Time to peak, half recovery time, and response amplitude normalized to basal fluorescence were analyzed for CatchER and D1ER citrine fluorescence ($\Delta F/F$). Asterisks indicate a statistically significant difference ($^*P < 0.01$). Values are mean ± SEM for 19 and 13 fibers expressing CatchER or D1ER FDB, respectively.

Table S1. Major parameters of genetically encoded ER Ca^{2+} sensors

	Ca^{2+} response	K_d (in situ), μM	Hill coefficient (*n*)	Calibration equation	Application in excitable cells	Measured resting $[Ca^{2+}]_{ER/SR}$
Cameleon1/E104Q	Monophasic	4.4	0.76	$[Ca^{2+}] = K'_d[(R - R_{min})/(R_{max} - R)]^{(1/n)}$ $K'_d = K_d(Sf2/Sb2)^{1/n}$	—	–/Saturated
Cameleon1/E31Q, YC4.3	Biphasic	0.8, 700 (0.039, 292)	1.5, 0.87 (0.57, 0.6)	$\%\Delta R = \{R_{max1}[Ca^{2+}]^{n1}/(K'_{d1}{}^{n1} + [Ca^{2+}]^{n1})\} + \{R_{max2}[Ca^{2+}]^{n2}/(K''_2{}^{n2} + [Ca^{2+}]^{n2})\}$	—	~200–700 μM
Split YC7.3	Monophasic	130	1.4	$[Ca^{2+}] = K'_d[(R - R_{min})/(R_{max} - R)]^{(1/n)}$ $K'_d = K_d(Sf2/Sb2)^{1/n}$	—	
D1ER	Biphasic	0.8, 60 (200)	1.18, 1.67	$\%\Delta R = \{R_{max1}[Ca^{2+}]^{n1}/(K'_{d1}{}^{n1} + [Ca^{2+}]^{n1})\} + \{R_{max2}[Ca^{2+}]^{n2}/(K'_{d2}{}^{n2} + [Ca^{2+}]^{n2})\}$	Yes	~100–300 μM
CatchER	Monophasic	180 (1,090)	(0.94)	$[Ca^{2+}] = K_d[(F - F_{min})/(F_{max} - F)]$	Yes	~300–800 μM